How to cite: *Angew. Chem. Int. Ed.* **2021**, *60*, 14954–14959
International Edition: doi.org/10.1002/anie.202100438
German Edition: doi.org/10.1002/ange.202100438

Metal-Peroxide Reactivity

Ligand-Constraint-Induced Peroxide Activation for Electrophilic Reactivity

Anirban Chandra, Mursaleem Ansari, Inés Monte-Pérez, Subrata Kundu, Gopalan Rajaraman, and Kallol Ray**

Abstract: *μ-1,2-peroxo-bridged diiron(III) intermediates* ***P*** *are proposed as reactive intermediates in various biological oxidation reactions. In sMMO,* ***P*** *acts as an electrophile, and performs hydrogen atom and oxygen atom transfers to electron-rich substrates. In cyanobacterial ADO, however,* ***P*** *is postulated to react by nucleophilic attack on electrophilic carbon atoms. In biomimetic studies, the ability of μ-1,2-peroxo-bridged dimetal complexes of Fe, Co, Ni and Cu to act as nucleophiles that effect deformylation of aldehydes is documented. By performing reactivity and theoretical studies on an end-on μ-1,2-peroxodicobalt(III) complex* ***1*** *involving a non-heme ligand system, L1, supported on a Sn_6O_6 stannoxane core, we now show that a peroxo-bridged dimetal complex can also be a reactive electrophile. The observed electrophilic chemistry, which is induced by the constraints provided by the Sn_6O_6 core, represents a new domain for metal–peroxide reactivity.*

Introduction

Binuclear non-heme metalloenzymes activate O_2 to carry out a variety of important biological processes.[1] These processes often involve the formation of a μ-1,2-peroxo-bridged bimetallic intermediate **P**, which is either further reduced to a bridging oxo intermediate or more generally directly involved in both electrophilic and nucleophilic reactions with various substrates.[2] In the diiron form of cyanobacterial aldehyde-deformylating oxygenases,[3] a peroxo-bridged diiron(III) complex is suggested to perform a nucleophilic attack on the carbonyl carbon of the substrate to form a $Fe_2^{III/III}$–peroxyhemiacetal complex, which undergoes reductive O–O bond cleavage that leads to C1–C2 radical fragmentation and formation of the alkane/alkene and formate products. In soluble methane monooxygenase (*s*MMO),[4a,b] on the other hand, the intermediate **P** undergoes a proton-promoted O–O bond scission and rearrangement of the diiron core to form a bis(μ-oxo)diiron(IV) unit, termed **Q**, that is directly responsible for the oxidation of methane to methanol. Detailed reactivity studies have suggested that **P** in *s*MMO also exhibits a unique ability to initiate electrophilic oxidation reactions (Scheme 1) directly via a two-electron or a hydride abstraction pathway,[4c–e] which is in contrast to the one-electron oxidation processes that are preferred by **Q**. In the arylamine oxygenase of the chloramphenicol biosynthesis (CmlI),[5] toluene 4-monooxygenase (T4MO),[6] Δ^9 desaturase (Δ^9D)[7] and 4-aminobenzoate N-oxygenase (AurF),[8] on the other hand, the μ-1,2-peroxo **P** intermediates are inactive towards substrates and require further activation for electrophilic reactions. In T4MO an intramolecular electron transfer in **P** leads to the formation of an $Fe^{II}Fe^{III}$–superoxide species as the active intermediate.[9] In Δ^9D, CmlI or in AurF, on the other hand, the activation process seems to involve the conversion of **P** to a new intermediate **P′**,[2,8c,10] whose structure has been controversially discussed as possessing either a μ-1,1- or μ-1,2-hydroperoxo bridge or a non-protonated peroxo structure having an additional water ligand. Overall, although the role of

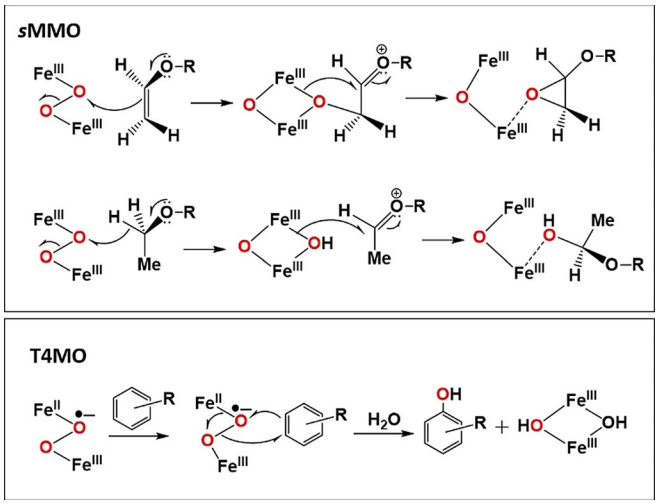

Scheme 1. Proposed peroxo intermediates for electrophilic reactivity in sMMO and T4MO.

[*] Dr. A. Chandra, Dr. I. Monte-Pérez, Dr. S. Kundu, Prof. Dr. K. Ray
Department of Chemistry
Humboldt-Universität zu Berlin
Brook-Taylor-Strasse 2, 12489 Berlin (Germany)
E-mail: kallol.ray@chemie.hu-berlin.de

M. Ansari, Prof. Dr. G. Rajaraman
Department of Chemistry
Indian Institute of Technology Bombay
Powai, Mumbai, Maharashtra, 400 076 (India)
E-mail: rajaraman@chem.iitb.ac.in

Supporting information and the ORCID identification number(s) for the author(s) of this article can be found under: https://doi.org/10.1002/anie.202100438.

enzymatic μ-1,2-peroxo-bridged bimetallic intermediate **P** intermediates for the oxidation of substrates containing C–H/O–H bonds has been suggested, the factors that lead to peroxide activation for electrophilic reactions are not properly understood.

In biomimetic studies, a number of mono- and di-nuclear metal–oxygen model complexes have been trapped and characterized allowing an assessment of the reactivity of the metal-bound oxo, (hydro)peroxo, and superoxo ligands.[11] These complexes displayed the ability to initiate a number of electrophilic and nucleophilic oxidative transformations that mimic the reactivity of the enzymatic systems. Whereas electrophilic reactions are generally associated with metal–oxo, hydroperoxo, and superoxo cores, metal–peroxo cores can mainly account for the nucleophilic reactivity. Metal–peroxo mediated electrophilic oxidation reactions are observed in extremely rare cases.[11o,12,13] For example, a mononuclear side-on manganese(III)–peroxo complex[12] is proposed to react with aldehydes through electrophilic hydrogen-atom transfer (HAT) reactions instead of the commonly proposed nucleophilic addition reaction. Additionally, side-on peroxo-bridged dicopper(II) cores[13] can also initiate oxidation of substrates containing C–H/O–H bonds; however, these intermediates are known to be in equilibrium with the bis(μ-oxo)dicopper(III) species in solution and the exact nature of the reactive intermediate responsible for the electrophilic reactions has proved to be ambiguous. To the best of our knowledge, no evidence for a μ-1,2-peroxo-bridged bimetallic intermediate that performs electrophilic C–H bond oxidation reactions has been reported to date. As such, no experimental verification of the postulated electrophilic reactivity of μ-1,2-peroxo-bridged diiron(III) intermediate **P** in *s*MMO exists. Herein, we describe our investigations into the electrophilic reactivity of a μ-1,2-peroxo-bridged bimetallic model complex toward intermolecular C–H and O–H bond activation reactions.

Results and Discussion

In a previous study, we reported the synthesis of a novel hexanucleating non-heme ligand system L1 (Scheme 2),[14] supported on a stannoxane core along with its iron(II) complex $\{[L1Fe_6]^{12+}\}$, which performed a rare O–O bond formation upon reaction with iodosobenzene to yield a superoxo complex, $\{[L1(Fe^{III}(O_2^{\bullet-})Fe^{II})_3]^{12+}\}$. The involvement of a μ-1,2-peroxo-bridged diiron(III) species was proposed, whose transient nature prevented its isolation. The replacement of the iron centers by cobalt led to a significant increase in the stability of the M-O-O-M core, which allowed the isolation of the $\{[L1(Co^{III}(O_2)Co^{III})_3]\}^{12+}$ complex **1** (Scheme 2) upon dioxygen activation of the hexanuclear cobalt complex $\{[L1Co_6]^{12+}\}$ in the temperature range −50 to 25 °C.[15] UV/Vis, resonance Raman, X-ray absorption spectroscopy, magnetic circular dichroism, and theoretical studies confirmed the presence of an antiferromagnetically coupled μ-1,2-peroxodicobalt(III) core in **1** with an $S=0$ ground state, where the O_2^{2-} units act as intramolecular bridge between the cobalt centers in $\{[L1Co_6]^{12+}\}$. The possibility of intermolecular dioxygen binding was excluded based on the non-dependence of the rate of formation of **1** on the concentration of $\{[L1Co_6]^{12+}\}$, as well as the O_2-titration experiments, which showed that three equivalents of O_2 were necessary for the complete formation of **1**. The formation of an intramolecularly bridged μ-1,2-peroxo-dicobalt(III) core was demonstrated to impose significant restraints on the conformational flexibility of the Co-binding arms of the stannoxane core, which made O_2-binding an entropically unfavorable process. This increasingly favored the dissociation of O_2 with increasing temperature.[15] The temperature dependence of the stability of **1** was reflected in the change in selectivity of the $\{[L1Co_6]^{12+}\}$-catalyzed O_2 reduction reaction from a preferential $4e^-/4H^+$ dioxygen reduction (to water) at −50 °C to a $2e^-/2H^+$ process (to hydrogen peroxide) at +25 °C. In the present study, we demonstrate that the constraints imposed by the stannoxane core of L1 also activate the peroxide core in **1** for electrophilic reactivity, thereby making **1** the only example of a μ-1,2-peroxo-bridged bimetallic complex known to date that is capable of C–H and O–H bond activation reactions.

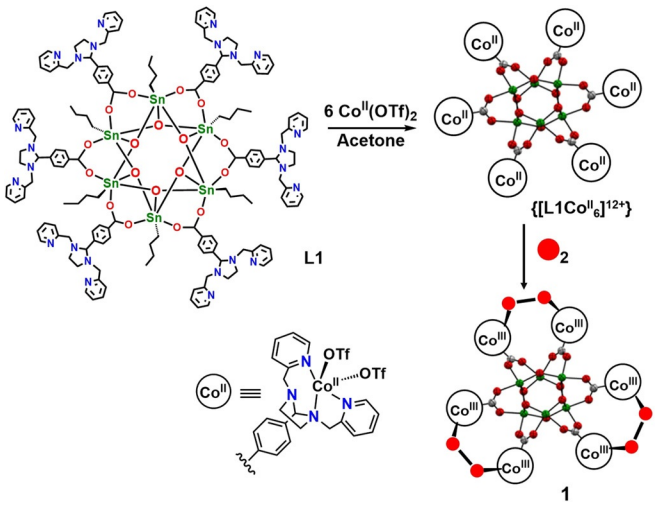

Scheme 2. The structure of the ligand and complexes used in the present work.

The electrophilic character of **1** was tested by the addition of 1-benzyl-1,4-dihydronicotinamide (BNAH), xanthene, dihydroanthracene (DHA), 1,4-cyclohexadiene (CHD), and fluorene to the preformed solutions of **1** in deaerated acetone at 25 °C, which resulted in the disappearance of the characteristic absorption band at 470 nm with a pseudo-first order decay profile (Figures 1 a,b for xanthene reaction; see SI Figures S1–S5 for the other substrates); the linear dependence of the pseudo-first order rate constants (k_{obs}) on substrate concentrations led us to determine the second-order rate constants (k_2). The k_2 values decrease with an increase in the C–H bond dissociation energies (BDE)[16] of the substrates. Figure 2 A shows a linear correlation between the $\log k_2'$ (where k_2' values are obtained by dividing the second-order rate constant k_2 by the number of equivalent target H atom in the substrates)[17] and the C–H BDE values of the substrates (Table S1), which supports C–H bond activation via a rate-determining HAT process. An analysis of the reaction mixture with GC–MS and/or NMR showed the

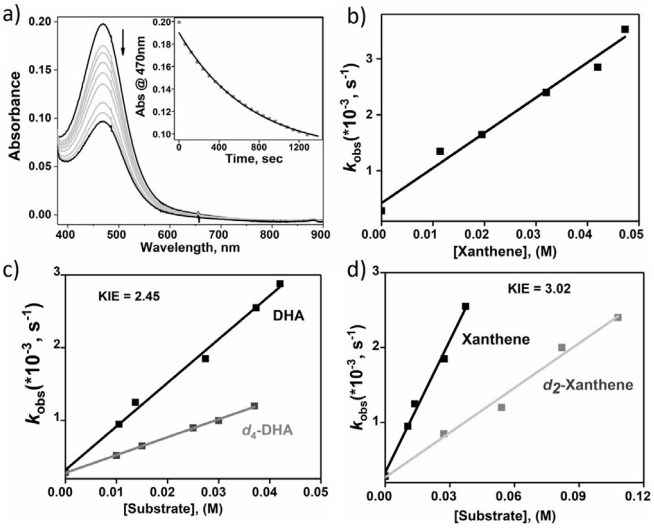

Figure 1. a) UV/Vis changes associated with the reaction of **1** (1.5×10^{-5} M) with xanthene (80 equiv); in the inset is shown the time trace of the decay of the 470 nm band and the pseudo-first order fit. b) Variation of the pseudo-first order rate constants with varying substrate concentrations and the linear plot to obtain the k_2 value. c) Determination of the KIE value for the reaction of **1** with DHA at 25 °C. d) Determination of the KIE value for the reaction of **1** with xanthene at 25 °C. The *y*-intercept in (b)–(d) corresponds to 2.8×10^{-4} s^{-1}, which is the self-decay of **1** at 25 °C.

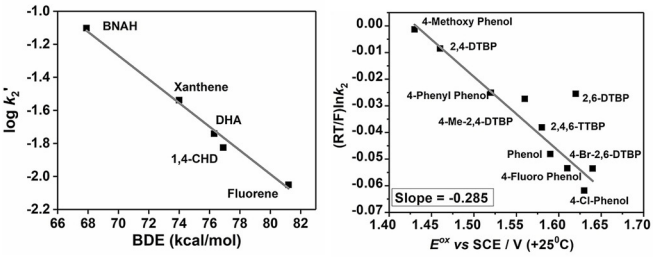

Figure 2. Left: plot of the logk_2′ vs. BDE for the reactions of **1** with different substrates at 25 °C; although the products in Table S1 correspond to more than one HAT reaction, the first HAT is approximated to be rate determining. Right: plot of $(RT/F)\ln k_2$ against the oxidation potentials (E_{ox}^0) of the substrates for the reaction of substituted ArOH with **1** at 25 °C.

formation of xanthone, anthracene, benzene, and 9-fluorenone, respectively, as the oxidation products (Figure S6–S9). Complex **1** also performed oxygen atom transfer (OAT) to PPh_3 to form Ph_3PO in 58% yield (Figure S10). The source of oxygen in the xanthone and Ph_3PO products turned out to be the Co-O-O-Co unit in **1**, which was shown by an ^{18}O-labeling experiment using ^{18}O-labeled **1**. Furthermore, the resultant solution is silent in the X-band EPR, which is consistent with the formation of Co^{III} products. Thus, each of the three Co-O-O-Co units in **1** acts as a one-electron oxidant; the incomplete mass balance may presumably be attributed to the non-involvement of all the three Co-O-O-Co units in oxidation reactions mediated by **1**.

Notably, cobalt–peroxo species are known to be nucleophilic oxidants[18a–e] and dicobalt–peroxo compounds are proposed as potential intermediates in water oxidation[18f,g] and dioxygen reduction reactions.[18h,i] However, no precedents of Co–peroxo-mediated intermolecular C–H and O–H bond activation reactions are known in the literature. Further mechanistic studies were therefore performed in order to confirm whether the Co^{III}-O_2-Co^{III} cores in **1** are directly responsible for the observed HAT and OAT reactions, or whether they can be attributed to minor amounts of $Co^{IV/V}$–O cores present in solution in equilibrium with the peroxo species. First, deuterium kinetic isotope effects (KIE) on the second-order rate constant k_2(C–H)/k_2(C–D) were measured for xanthene and DHA. The determined KIE values of 3.02 and 2.45, respectively, (Figure 1c,d) for DHA and xanthene are smaller than the KIE values obtained for most metal–oxo-mediated HAT reactions (7–25);[11,19] in particular, large KIE values of 13 and 8 have been recently reported for $[(TAML)Co^{IV}(O)(Sc(CF_3SO_2)_3]$ (TAML = tetraamido macrocyclic ligand)- and $[(13\text{-}TMC)Co^{IV}(O)]^{2+}$ (13-TMC = 1,4,7,10-tetramethyl-1,4,7,10-tetraazacyclotridecane)-mediated HAT reactions.[20] One indirect method frequently used to confirm the involvement of a metal–oxo core in solution is to carry out the oxidation reactions in the presence of ^{18}O-labeled water ($H_2{}^{18}O$), since metal–oxo complexes can exchange their O-atom with ^{18}O-labeled water prior to the O-atom transfer to organic substrates.[21] In order to determine whether or not a $Co^{IV/V}$–O species was forming in solution and was responsible for the observed electrophilic reactivity, **2** was set to react with PPh_3 in acetone in the presence of 0.01 mL of $H_2{}^{18}O$. Although OAT to PPh_3 also occurs in the presence of $H_2{}^{18}O$ (Figure S10), the analysis of the reaction mixture showed no incorporation of ^{18}O into the $OPPh_3$ product.

For a better understanding of the electrophilic reactivity of **1**, we investigated its reactivity with different substituted phenols (Figures S11–S21) and provide deeper insights into the O–H bond activation mechanism towards substituted phenols by applying the Brønsted/Tafel analogy published by Ram and Hupp[22] for electron transfer processes. Kinetic isotope labeling studies on the oxidation of 2,6-Di-*tert*-butyl-4-methoxy phenol (4-OMe-2,6-DTBP) and phenol by **1** yielded KIE values of 3.09 and 2.93, respectively, corroborating the involvement of proton transfer in the rate-determining step (Figure S11). Furthermore, k_2 values (Table S2) were determined for the reactions of **1** with different substituted phenols (ArOH), which when correlated to the ArOH/ArOH$^+$ potentials (E^{ox}) of the phenols afford a good linear correlation for the $(RT/F)\ln k_2$ versus E^{ox} plot with a slope of −0.29 (Figure 2, right). A one-step HAT mechanism (Scheme 3) can

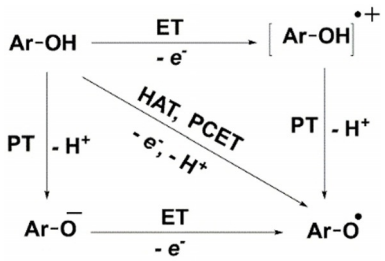

Scheme 3. Possible reaction pathways for the oxidation of phenols.

be excluded based on the dependence of k_2 on E^{ox}. The observed slope of −0.29 is also inconsistent with a concerted proton-coupled electron transfer (PCET) mechanism, for which a slope between −0.5 and −1.0 is expected.[23,24] The stronger than expected dependence on oxidation potential may imply uncoupled proton (PT) and electron (ET) transfers (Scheme 3) with a partial transfer of charge from hydrogen donors to the Co-O-O-Co unit in **1**, as reported previously in the literature.[23b,24] This would also be consistent with the observed weak correlation of the KIE values to the O–H/C–H BDEs (Figure S11).

Analysis of the reaction mixtures for 2,6-di-*tert*-butylphenol (2,6-DTBP), 4-OMe-2,6-DTBP, and 2,4,6-tri-*tert*-butylphenol (2,4,6-TTBP) demonstrated the formation of the corresponding benzoquinone products in 30–40% yield (Table S2; Figures S22–S24). When ^{18}O-labeled **1** was used, significant ^{18}O-atom incorporation occurred in the resulting benzoquinone, so that the oxygen atom incorporated into the oxidized product originates from **1** (Figures S22, S24). Furthermore, in the case of the reactions of **1** with 2,4,6-TTBP and 4-Br-2,6-DTBP the formation of the corresponding phenoxyl radicals (yield: 22% for 2,4,6-TTBP and 15% for 4-Br-2,6-DTBP)[25] with UV/Vis absorption bands at approximately 400 and 420 nm (Figures S13 and S20) and sharp EPR signals (Figure S25) at $g = 2.00$ were detected. Based on these results, the reaction of **1** with phenols may be explained by a mechanism depicted in Scheme S1, which is reminiscent of the reaction path proposed previously for selected cobalt–, nickel– and copper–superoxo systems.[23b,26] The phenoxyl radical formed after the initial transfer of hydrogen atom to the Co-O-O-Co unit in **1** may react with a second Co-O-O-Co core to generate a cobalt(III)aryl peroxo species, which upon O–O bond cleavage will yield a benzoquinone product incorporating a new oxygen atom coming from the peroxo moiety. Although the present study lacks any direct evidence of the formation of the cobalt(III)aryl peroxo species, its involvement is tentatively assigned based on the detection of formaldehyde by employing the Nash assay[27] in the reaction of **1** with 4-OMe-2,6-DTBP (Figure S26). Furthermore, the resultant solution lacks any cobalt-based signal in the X-band EPR, which is consistent with the formation of the Co^{III} products.

DFT calculations were performed to obtain insights into the origin of the unique electrophilic reactivity of **1**. In order to approximate the constraints provided by the stannoxane core, we designed a simplified end-on μ-1,2-peroxodicobalt(III) system ($\mathbf{1}_{con}$), where the distance between the two ligand carbonyl carbons was fixed to 4.044 Å, based on the structure of L1 (Figure 3). The second structure ($\mathbf{1}_{uncon}$) is optimized without any constraints, and may model the large number of previously reported μ-1,2-peroxodicobalt(III) systems,[18a,f–i] for which no electrophilic reactivities were observed. The Co^{III} atoms in both $\mathbf{1}_{con}$ and $\mathbf{1}_{uncon}$ are five-coordinate with a bound triflate anion ($S_{Co} = 1$) and found to be antiferromagnetically coupled leading to a $S_T = 0$ ground state as estimated earlier,[15] and hence we focused our attention particularly on these broken-symmetry states corresponding to a $S_T = 0$ ground state. Calculations reveal that $\mathbf{1}_{con}$ is thermodynamically more stable than $\mathbf{1}_{uncon}$ by 13.6 kJ mol^{-1}.

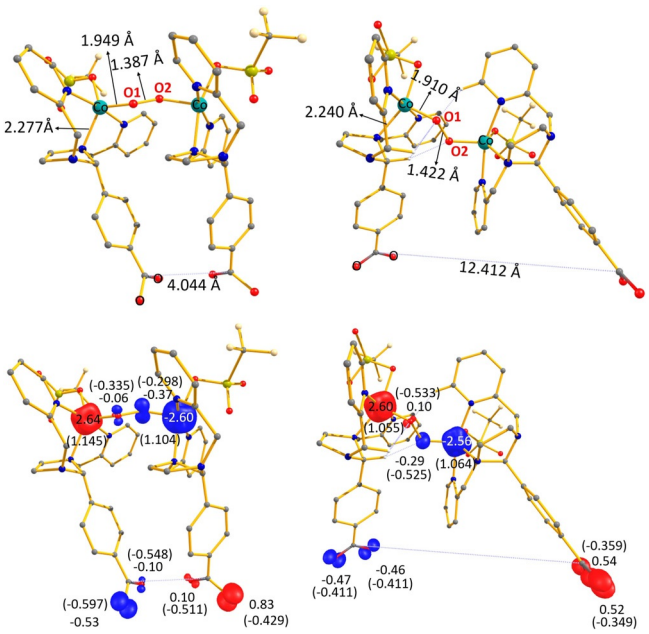

Figure 3. Top: optimized structures of $\mathbf{1}_{con}$ (left) and $\mathbf{1}_{uncon}$ (right). Bottom: the corresponding spin density plots of $\mathbf{1}_{con}$ (left) and $\mathbf{1}_{uncon}$ (right). The values given in parenthesis are the corresponding NPA charges on the particular atoms.

Notably, the calculated O–O bond length in $\mathbf{1}_{con}$ is significantly shorter than $\mathbf{1}_{uncon}$ (Figure 3, top; 1.387 Å vs. 1.422 Å; see also Figure S27). A closer look at the HOMO of $\mathbf{1}_{con}$ reveals a strong donation of π^*(O–O) bond to the Co-based d-orbitals. As explained previously[11n,o] this donation strengthens the O–O bond and increases the electrophilicity of the O_2^{2-} unit. Notably, the calculated vibrational frequency for $\mathbf{1}_{con}$ with $\tilde{\nu}$(O–O) at 894 cm^{-1} is in good agreement with the experiment ($\tilde{\nu}$(O–O) of 878 cm^{-1}). For $\mathbf{1}_{uncon}$, the computed $\tilde{\nu}$(O–O) vibration is found to be 865 cm^{-1}, supporting a weaker O–O bond. To quantify this π^*(O–O)→Co(d) donation, we have performed natural bond orbital (NBO) second-order perturbation theory analysis (Figure S28),[28] which reveals two strong π^*(O–O)→Co(d) donations stabilized by 144.7 kJ mol^{-1} and 46.8 kJ mol^{-1}, respectively, for $\mathbf{1}_{con}$. For $\mathbf{1}_{uncon}$, on the other hand, only one π^*(O–O)→Co d-based orbital interaction at 48.5 kJ mol^{-1} is detected. Notably, the donation from π^*(O–O) to Co-d based orbitals, and the O–O distances in $\mathbf{1}_{con}$ and $\mathbf{1}_{uncon}$ can be correlated to their Co^{III}–N-imidazolidinyl amine and Co–O distances of the $_{amine}$N-Co-O-O-Co-N$_{amine}$ core. The constraint provided by the stannoxane core in $\mathbf{1}_{con}$ makes the Co^{III}–N_{amine} bond at 2.277 Å and Co–O distance at 1.949 Å longer relative to that in $\mathbf{1}_{uncon}$ (2.240 Å and 1.910 Å, respectively); this makes the Co^{III} center in $\mathbf{1}_{con}$ more Lewis-acidic, thereby accounting for the stronger π^*(O–O) to Co(d) donation. NBO population analysis also affirms that the {O_2} moiety in $\mathbf{1}_{con}$ possesses approximately 0.43 electrons less as compared to $\mathbf{1}_{uncon}$ (see Table S3). The difference in electronic structure imposed by the structural constraints is also reflected in various observables such as spin density and charges. Although the spin density (Figure 3, bottom) at the metal center is similar for both $\mathbf{1}_{con}$ and $\mathbf{1}_{uncon}$, there is some subtle difference in the spin density at the {O_2}

moiety. Particularly in $\mathbf{1}_{con}$, the net $\{O_2\}$ moiety spin density is estimated to be −0.43 (−0.06 at **O1** and −0.37 at **O2**), while in the case of $\mathbf{1}_{uncon}$, it is found to be −0.19 (0.10 at **O1** and −0.29 at **O2**), suggesting a higher radical character of the bridging oxygens in $\mathbf{1}_{con}$ and hence a greater ability to abstract a hydrogen atom from C−H/O−H bonds (see Figure 3, bottom).[29] Additionally, we have also carefully looked at the NPA charges, which are very important for understanding the electrophilic and nucleophilic character of the $\{O_2\}$ moiety. The oxygen atoms were found to have a significant negative charge in $\mathbf{1}_{uncon}$ compared to $\mathbf{1}_{con}$ ($Q_C(OO) = -0.633$ (−0.335 at **O1** and −0.298 at **O2**) for $\mathbf{1}_{con}$ and $Q_C(OO) = -1.058$ (−0.533 at **O1** and −0.525 at **O2**) for $\mathbf{1}_{uncon}$; Figure 3, bottom), further confirming the more electrophilic character of $\mathbf{1}_{con}$.

The space-filling models of the optimized structures are shown in Figure S29. The $\{O_2\}$ moiety in $\mathbf{1}_{uncon}$ is sterically hindered and less accessible to the substrates than that in $\mathbf{1}_{con,}$ where the clear approach of the substrate to the $\{O_2\}$ moiety is feasible. Furthermore, in $\mathbf{1}_{uncon}$, the pyridine rings are tilted towards the $\{O_2\}$ moiety due to the presence of two strong C−H···O interactions between the $\{O_2\}$ moiety and the hydrogen atoms of the pyridine rings and the amine groups (Figure S27). To further understand the electrophilic reactivity of **1**, we investigated the formation of the reactant complex **1-RC** for the reactions of $\mathbf{1}_{con}/\mathbf{1}_{uncon}$ with DHA (Figures S30–S32). It was found to be exothermic in both cases, with $\mathbf{1}_{con}$-**RC** being more stable ($-47.7\ kJ\,mol^{-1}$) than $\mathbf{1}_{uncon}$-**RC** ($-26.7\ kJ\,mol^{-1}$) with respect to the free reactants. Furthermore, in $\mathbf{1}_{con}$-**RC**, the DHA approaches the $\{O_2\}$ moiety very closely with the C−H···O−O distance of 2.577 Å (Figures S30 and S31) that leads to a very strong interaction of the σ(C−H) bond with the π^*(O−O) and Co(d) orbitals, as also revealed by the nature of the HOMO (Figure S32). In $\mathbf{1}_{uncon}$-**RC**, on the other hand, the closest C−H···O−O distance is found to be 5.038 Å with no major interaction between the π^*(O−O) and Co(d) orbitals. A closer look at the Mulliken charges (Figure S33) reveals a decrease in the charges of the carbon and hydrogen atoms of DHA that are involved in interaction with the $\{O_2\}$ moiety compared to free DHA in $\mathbf{1}_{con}$-**RC** (from a value of −0.156 in free DHA to a value of −0.082 in $\mathbf{1}_{con}$-**RC** for C and from 0.105 in free DHA to 0.049 in $\mathbf{1}_{con}$-**RC** for H). This interaction also alters the spin density at the interacting oxygen atom (**O2**, Table S4) from −0.37 in $\mathbf{1}_{con}$ to +0.31 in $\mathbf{1}_{con}$-**RC**. In contrast, for $\mathbf{1}_{uncon}$-**RC** the observed changes relative to $\mathbf{1}_{uncon}$ are very small or negligible (see Figure S33 and Table S4). This is consistent with a partial transfer of charge from DHA to the Co-O-O-Co unit in $\mathbf{1}_{con}$-**R** (and not in $\mathbf{1}_{uncon}$-**RC**), which is in line with the experimentally observed mechanism for complex **1**-mediated O−H bond activation reactions (Figure 2B).

Conclusion

The μ-1,2-peroxo **P** intermediates in diiron enzymes are in general inactive towards substrates and require activation by protonation for electrophilic oxidation reactions like HAT and OAT reactions. However, **P** from *s*MMO has been shown to oxidize electron-rich substrates like ethyl vinyl ether, diethyl ether, and propylene, and the peroxide activation mechanism is not well understood. In the present work, we now report a μ-1,2-peroxo dicobalt(III) complex **1** that is capable of performing HAT from substrates containing C−H and O−H bonds and OAT to PPh_3. The electrophilic reactivity of **1** is in sharp contrast to the previous reports of biomimetic μ-1,2-peroxo dimetal complexes of Fe, Co, Ni, and Cu that all act as nucleophiles and effect the deformylation of aldehydes. DFT studies suggest that a strong O_2^{2-}-to-Co^{III} π-donation, which can be attributed to the constraint provided by the stannoxane core that makes the Co^{III} centers Lewis acidic, contributes to the unique electrophilicity of **1**. Whether or not a similar peroxide activation mechanism for electrophilic oxidation reactions is applicable for the μ-1,2-peroxo diiron(III) intermediate in the catalytic cycle of *s*MMO is now a particularly intriguing question.

Acknowledgements

This work was funded by the Deutsche Forschungsgemeinschaft (DFG, German Research Foundation) under Germany's Excellence Strategy—EXC 2008–390540038—UniSysCat to K.R. G.R. would like to thank DST (DST/SJF/CSA-03/2018-10) and SERB (CRG/2018/000430; SB/SJF/2019-20/12; SPR/2019/001145) for funding. Open access funding enabled and organized by Projekt DEAL.

Conflict of interest

The authors declare no conflict of interest.

Keywords: C−H bond oxidations · electrophilic reactions · phenol oxidations · reaction mechanism · μ-1,2-peroxo dicobalt(III)

[1] a) A. J. Jasniewski, L. Que, Jr., *Chem. Rev.* **2018**, *118*, 2554–2592; b) E. I. Solomon, K. Park, *J. Biol. Inorg. Chem.* **2016**, *21*, 575–588; c) C. Krebs, J. M. Bollinger, Jr., S. J. Booker, *Curr. Opin. Chem. Biol.* **2011**, *15*, 291.

[2] a) A. D. Bochevarov, J. N. Li, W. J. Song, R. A. Friesner, S. J. Lippard, *J. Am. Chem. Soc.* **2011**, *133*, 7384–7397; b) K. P. Jensen, C. B. Bell, M. D. Clay, E. I. Solomon, *J. Am. Chem. Soc.* **2009**, *131*, 12155–12171; c) E. I. Solomon, T. C. Brunold, M. I. Davis, J. N. Kemsley, S.-K. Lee, N. Lehnert, F. Neese, A. J. Skulan, Y.-S. Yang, J. Zhou, *Chem. Rev.* **2000**, *100*, 235; d) M. Srnec, T. A. Rokob, J. K. Schwartz, Y. Kwak, L. Rulísek, E. I. Solomon, *Inorg. Chem.* **2012**, *51*, 2806–2820.

[3] a) M. E. Pandelia, N. Li, H. Nørgaard, D. M. Warui, L. J. Rajakovich, W. Chang, S. J. Booker, C. Krebs, J. M. Bollinger, Jr., *J. Am. Chem. Soc.* **2013**, *135*, 15801; b) N. Li, H. Nørgaard, D. M. Warui, S. J. Booker, C. Krebs, J. M. Bollinger, Jr., *J. Am. Chem. Soc.* **2011**, *133*, 6158.

[4] a) K. E. Liu, D. Wang, B. H. Huynh, D. E. Edmondson, A. Salifoglou, S. J. Lippard, *J. Am. Chem. Soc.* **1994**, *116*, 7465–7466; b) A. M. Valentine, S. S. Stahl, S. J. Lippard, *J. Am. Chem. Soc.* **1999**, *121*, 3876–3887; c) L. Shu, J. C. Nesheim, K. Kauffmann, E. Münck, J. D. Lipscomb, L. Que, Jr., *Science* **1997**, *275*, 515–518; d) S.-K. Lee, B. G. Fox, W. A. Froland, J. D.

Lipscomb, E. Münck, *J. Am. Chem. Soc.* **1993**, *115*, 6450 – 6451; e) L. G. Beauvais, S. J. Lippard, *J. Am. Chem. Soc.* **2005**, *127*, 7370 – 7378.

[5] a) T. M. Makris, V. V. Vu, K. K. Meier, A. J. Komor, B. S. Rivard, E. Münck, L. Que, Jr., J. D. Lipscomb, *J. Am. Chem. Soc.* **2015**, *137*, 1608 – 1617; b) C. J. Knoot, E. G. Kovaleva, J. D. Lipscomb, *J. Biol. Inorg. Chem.* **2016**, *21*, 589 – 603; c) A. J. Jasniewski, A. J. Komor, J. D. Lipscomb, L. Que, Jr., *J. Am. Chem. Soc.* **2017**, *139*, 10472 – 10485.

[6] a) J. K. Schwartz, P.-p. Wei, K. H. Mitchell, B. G. Fox, E. I. Solomon, *J. Am. Chem. Soc.* **2008**, *130*, 7098 – 7109; b) L. J. Bailey, J. G. McCoy, G. N. Phillips, Jr., B. G. Fox, *Proc. Natl. Acad. Sci. USA* **2008**, *105*, 19194 – 19198.

[7] a) J. A. Broadwater, J. Ai, T. M. Loehr, J. Sanders-Loehr, B. G. Fox, *Biochemistry* **1998**, *37*, 14664 – 14671.

[8] a) V. K. Korboukh, N. Li, E. W. Barr, J. M. Bollinger, Jr., C. Krebs, *J. Am. Chem. Soc.* **2009**, *131*, 13608 – 13609; b) N. Li, V. K. Korboukh, C. Krebs, J. M. Bollinger, Jr., *Proc. Natl. Acad. Sci. USA* **2010**, *107*, 15722; c) K. Park, N. Li, Y. Kwak, M. Srnec, C. B. Bell, L. V. Liu, S. D. Wong, Y. Yoda, S. Kitao, M. Seto, M. Hu, J. Zhao, C. Krebs, J. M. Bollinger, E. I. Solomon, *J. Am. Chem. Soc.* **2017**, *139*, 7062 – 7070.

[9] J. F. Acheson, L. J. Bailey, T. C. Brunold, B. G. Fox, *Nature* **2017**, *544*, 191 – 195.

[10] P. Jayapal, A. Ansari, G. Rajaraman, *Inorg. Chem.* **2015**, *54*, 11077.

[11] a) M. Puri, L. Que, Jr., *Acc. Chem. Res.* **2015**, *48*, 2443; b) W. Nam, *Acc. Chem. Res.* **2015**, *48*, 2415; c) T. P. Zimmermann, N. Orth, S. Finke, T. Limpke, A. Stammler, H. Bögge, S. Walleck, I. Ivanovic-Burmazovic, T. Glaser, *Inorg. Chem.* **2020**, *59*, 15563; d) L. Que, Jr., W. B. Tolman, *Angew. Chem. Int. Ed.* **2002**, *41*, 1114; *Angew. Chem.* **2002**, *114*, 1160; e) E. Y. Tshuva, S. J. Lippard, *Chem. Rev.* **2004**, *104*, 987; f) J. J. D. Sacramento, D. P. Goldberg, *Acc. Chem. Res.* **2018**, *51*, 2641; g) Y. Liu, T.-C. Lau, *J. Am. Chem. Soc.* **2019**, *141*, 3755; h) S. M. Adam, G. B. Wijeratne, P. J. Rogler, D. E. Diaz, D. A. Quist, J. J. Liu, K. D. Karlin, *Chem. Rev.* **2018**, *118*, 10840; i) D. A. Quist, D. E. Diaz, J. J. Liu, K. D. Karlin, *J. Biol. Inorg. Chem.* **2017**, *22*, 253; j) J. Cho, S. Jeon, S. A. Wilson, L. V. Liu, E. A. Kang, J. J. Braymer, M. H. Lim, B. Hedman, K. O. Hodgson, J. S. Valentine, E. I. Solomon, W. Nam, *Nature* **2011**, *478*, 502; k) K. Dalle, T. Gruene, S. Dechert, S. Demeshko, F. Meyer, *J. Am. Chem. Soc.* **2014**, *136*, 7428; l) P. C. Duan, D. H. Manz, S. Dechert, S. Demeshko, F. Meyer, *J. Am. Chem. Soc.* **2018**, *140*, 4929; m) N. Zhao, A. S. Filatov, J. Xie, E. A. Hill, A. Y. Rogachev, J. S. Anderson, *J. Am. Chem. Soc.* **2020**, *142*, 21634; n) J. A. Rees, V. Martin-Diaconescu, J. A. Kovacs, S. DeBeer, *Inorg. Chem.* **2015**, *54*, 6410; o) M. K. Coggins, V. Martin-Diaconescu, S. DeBeer, J. A. Kovacs, *J. Am. Chem. Soc.* **2013**, *135*, 4260.

[12] P. Barman, F. G. C. Reinhard, U. K. Bagha, D. Kumar, C. V. Sastri, S. P. de Visser, *Angew. Chem. Int. Ed.* **2019**, *58*, 10639 – 10643; *Angew. Chem.* **2019**, *131*, 10749 – 10753.

[13] a) C. E. Elwell, N. L. Gagnon, B. D. Neisen, D. Dhar, A. D. Spaeth, G. M. Yee, W. B. Tolman, *Chem. Rev.* **2017**, *117*, 2059; b) L. M. Mirica, M. Vance, D. J. Rudd, B. Hedman, K. O. Hodgson, E. I. Solomon, T. D. P. Stack, *Science* **2005**, *308*, 1890; c) M. Rolff, J. Schottenheim, H. Decker, F. Tuczek, *Chem. Soc. Rev.* **2011**, *40*, 4077; d) C. Würtele, O. Sander, V. Lutz, T. Waitz, F. Tuczek, S. Schindler, *J. Am. Chem. Soc.* **2009**, *131*, 7544; e) M. Rolff, F. Tuczek, *Angew. Chem. Int. Ed.* **2008**, *47*, 2344; *Angew. Chem.* **2008**, *120*, 2378.

[14] S. Kundu, E. Matito, S. Walleck, F. F. Pfaff, F. Heims, B. Rábay, J. M. Luis, A. Company, B. Braun, T. Glaser, K. Ray, *Chem. Eur. J.* **2012**, *18*, 2787 – 2791.

[15] I. Monte-Pérez, S. Kundu, A. Chandra, K. E. Craigo, P. Chernev, U. Kuhlmann, H. Dau, P. Hildebrandt, C. Greco, C. Van Stappen, N. Lehnert, K. Ray, *J. Am. Chem. Soc.* **2017**, *139*, 15033 – 15042.

[16] Y.-R. Luo, *Comprehensive Handbook of Chemical Bond Energies*, CRC Press, Boca Raton, FL, **2007**.

[17] J. M. Mayer, *Acc. Chem. Res.* **2011**, *44*, 36 – 46.

[18] a) A. T. Fiedler, A. A. Fischer, *J. Biol. Inorg. Chem.* **2017**, *22*, 407; b) T. Corona, S. K. Padamati, F. Acuña-Parés, C. Duboc, W. R. Browne, A. Company, *Chem. Commun.* **2017**, *53*, 11782; c) X. Hu, I. Castro-Rodriguez, K. Meyer, *J. Am. Chem. Soc.* **2004**, *126*, 13464; d) Y. Jo, J. Annaraj, M. S. Seo, Y.-M. Lee, S. Y. Kim, J. Cho, W. Nam, *J. Inorg. Biochem.* **2008**, *102*, 2155; e) J. Cho, R. Sarangi, H. Y. Kang, J. Y. Lee, M. Kubo, T. Ogura, E. I. Solomon, W. Nam, *J. Am. Chem. Soc.* **2010**, *132*, 16977; f) C. Gimbert-Suriñach, D. Moonshiram, L. Francàs, N. Planas, V. Bernales, F. Bozoglian, A. Guda, L. Mognon, I. López, M. A. Hoque, L. Gagliardi, C. J. Cramer, A. Llobet, *J. Am. Chem. Soc.* **2016**, *138*, 15291; g) M. L. Rigsby, S. Mandal, W. Nam, L. C. Spencer, A. Llobet, S. S. Stahl, *Chem. Sci.* **2012**, *3*, 3058; h) S. Fukuzumi, S. Mandal, K. Mase, K. Ohkubo, H. Park, J. Benet-Buchholz, W. Nam, A. Llobet, *J. Am. Chem. Soc.* **2012**, *134*, 9906; i) C.-C. Wang, H.-C. Chang, Y.-C. Lai, H. Fang, C.-C. Li, H.-K. Hsu, Z.-Y. Li, T.-S. Lin, T.-S. Kuo, F. Neese, S. Ye, Y.-W. Chiang, M.-L. Tsai, W.-F. Liaw, W.-Z. Lee, *J. Am. Chem. Soc.* **2016**, *138*, 14186.

[19] K. Gunay, A. Theopold, *Chem. Rev.* **2010**, *110*, 1060 – 1081.

[20] a) S. Hong, F. F. Pfaff, E. Kwon, Y. Wang, M. S. Seo, E. Bill, K. Ray, W. Nam, *Angew. Chem. Int. Ed.* **2014**, *53*, 10403 – 10407; *Angew. Chem.* **2014**, *126*, 10571 – 10575; b) B. Wang, Y.-M. Lee, W.-Y. Tcho, S. Tussupbayev, S.-T. Kim, Y. Kim, M. S. Seo, K.-B. Cho, Y. Dede, B. C. Keegan, T. Ogura, S. H. Kim, T. Ohta, M. H. Baik, K. Ray, J. Shearer, W. Nam, *Nat. Commun.* **2017**, *8*, 14839.

[21] I. Prat, A. Company, V. Postils, X. Ribas, L. Que, Jr., J. M. Luis, M. Costas, *Chem. Eur. J.* **2013**, *19*, 6724 – 6738.

[22] M. S. Ram, J. T. Hupp, *J. Phys. Chem.* **1990**, *94*, 2378 – 2380.

[23] a) M. H. V. Huynh, T. J. Meyer, *Chem. Rev.* **2007**, *107*, 5004 – 5064; b) J. Y. Lee, R. L. Peterson, K. Ohkubo, I. Garcia-Bosch, R. A. Himes, J. Woertink, C. D. Moore, E. I. Solomon, S. Fukuzumi, K. D. Karlin, *J. Am. Chem. Soc.* **2014**, *136*, 9925 – 9937.

[24] a) J. B. Guttenplan, S. G. Cohen, *J. Am. Chem. Soc.* **1972**, *94*, 4040; b) P. J. Wagner, H. M. H. Lam, *J. Am. Chem. Soc.* **1980**, *102*, 4167.

[25] T. Wu, S. N. MacMillan, K. Rajabimoghadam, M. A. Siegler, K. M. Lancaster, I. Garcia-Bosch, *J. Am. Chem. Soc.* **2020**, *142*, 12265.

[26] a) A. Nishinaga, H. Tomita, T. Matsuura, *Tetrahedron Lett.* **1980**, *21*, 3407 – 3408; b) A. Nishinaga, H. Tomita, K. Nishizawa, T. Matsuura, S. Ooi, K. Hirotsu, *J. Chem. Soc. Dalton Trans.* **1981**, 1504 – 1514; c) A. Company, S. Yao, K. Ray, M. Driess, *Chem. Eur. J.* **2010**, *16*, 9669 – 9675; d) D. Maiti, H. C. Fry, J. S. Woertink, M. A. Vance, E. I. Solomon, K. D. Karlin, *J. Am. Chem. Soc.* **2007**, *129*, 264 – 265.

[27] T. Nash, *Biochem. J.* **1953**, *55*, 416 – 421.

[28] A. E. Reed, L. A. Curtiss, F. Weinhold, *Chem. Rev.* **1988**, *88*, 899.

[29] a) H. Schwarz, *Angew. Chem. Int. Ed.* **2011**, *50*, 10096 – 10115; *Angew. Chem.* **2011**, *123*, 10276 – 10297; b) N. Dietl, M. Schlangen, H. Schwarz, *Angew. Chem. Int. Ed.* **2012**, *51*, 5544 – 5555; *Angew. Chem.* **2012**, *124*, 5638 – 5650; c) C. Geng, J. Li, T. Weiske, H. Schwarz, *Chem. Eur. J.* **2019**, *25*, 12940 – 12945; d) M. Jaccob, A. Ansari, B. Pandey, G. Rajaraman, *Dalton Trans.* **2013**, *42*, 16518 – 16526; e) M. Ansari, D. Senthilnathan, G. Rajaraman, *Chem. Sci.* **2020**, *11*, 10669.

Manuscript received: January 11, 2021
Revised manuscript received: March 26, 2021
Accepted manuscript online: April 11, 2021
Version of record online: May 28, 2021

